Article

SOURCE DATA | TRANSPARENT PROCESS | OPEN ACCESS

THE EMBO JOURNAL

Notch and EGFR regulate apoptosis in progenitor cells to ensure gut homeostasis in *Drosophila*

Tobias Reiff[†,§], Zeus A Antonello[‡,§], Esther Ballesta-Illán, Laura Mira, Salvador Sala, Maria Navarro, Luis M Martinez & Maria Dominguez[*]

Abstract

The regenerative activity of adult stem cells carries a risk of cancer, particularly in highly renewable tissues. Members of the family of inhibitor of apoptosis proteins (IAPs) inhibit caspases and cell death, and are often deregulated in adult cancers; however, their roles in normal adult tissue homeostasis are unclear. Here, we show that regulation of the number of enterocyte-committed progenitor (enteroblast) cells in the adult *Drosophila* involves a caspase-mediated physiological apoptosis, which adaptively eliminates excess enteroblast cells produced by intestinal stem cells (ISCs) and, when blocked, can also lead to tumorigenesis. Importantly, we found that *Diap1* is expressed by enteroblast cells and that loss and gain of *Diap1* led to changes in enteroblast numbers. We also found that antagonistic interplay between Notch and EGFR signalling governs enteroblast life/death decisions via the Klumpfuss/WT1 and Lozenge/RUNX transcription regulators, which also regulate enteroblast differentiation and cell fate plasticity. These data provide new insights into how caspases drive adult tissue renewal and protect against the formation of tumours.

Keywords caspase; intestinal enteroblast; Klumpfuss/WT1; Lozenge/RUNX; physiological apoptosis

Subject Categories Autophagy & Cell Death; Development & Differentiation; Stem Cells & Regenerative Medicine

DOI 10.15252/embj.2018101346 | Received 11 December 2018 | Revised 20 July 2019 | Accepted 1 August 2019 | Published online 30 September 2019

The EMBO Journal (2019) 38: e101346

Introduction

The *Drosophila* intestinal epithelium is completely renewed several times during its 40–50 days of adult life in a process that takes 1–3 weeks under normal homeostatic self-renewal (Ohlstein & Spradling, 2007; Jiang *et al*, 2009; Antonello *et al*, 2015). However, after overt damage, it is renewed in just 2–3 days (Ohlstein & Spradling, 2007; Buchon *et al*, 2009; Jiang *et al*, 2009). The wide range of physiological turnover time reflects the stochastic damage of absorptive enterocytes (ECs)—the main cells in the intestinal epithelium (Biteau *et al*, 2011; Jiang & Edgar, 2011)—by exposure to pathogens and toxins present in food and chemicals and physical stress. The intestine also contains secretory enteroendocrine (EE) cells, which constitute only 10% of the intestinal population and renew themselves at a slower rate than ECs (de Navascués *et al*, 2012; Sallé *et al*, 2017; Parasram *et al*, 2018). Intestinal cell turnover is sustained by a small population of ISCs scattered throughout the epithelium that, as observed in other high-turnover epithelia in mammals (Simons & Clevers, 2011), divide regularly and produce, with each division, one cell that differentiates and one that remains undifferentiated. The renewed ISCs will divide in the same way to produce a new cell stem and a cell committed towards the same lineage as the previous division or into the other intestinal cell type (e.g. Micchelli & Perrimon, 2006; Ohlstein & Spradling, 2006, 2007; Jiang *et al*, 2009; Beehler-Evans & Micchelli, 2015; Chen *et al*, 2018); or it may divide symmetrically to expand the number of ISCs (O'Brien *et al*, 2011; de Navascués *et al*, 2012). However, in the highly renewing intestine, stem cells must operate rapidly and efficiently by providing enough new cells to replenish daily tissue demand. Moreover, since multipotent ISCs have different options in terms of cell lineage, an important unanswered question is how individual stem cells rapidly and adaptively produce the distinct tissue cell types at the right number to sustain tissue homeostasis in the short- and long-term.

In *Drosophila*, the intestine contains only two types of differentiated cells, the ECs and the enteroendocrine cells (ee). The commitment of enteroblasts (EBs) to produce ECs is relatively simple and requires the Delta (Dl)-Notch (N) signalling activation between the daughter cell that remains a stem cell and the daughter cell that becomes the committed progenitor cell (Ohlstein & Spradling, 2007; Perdigoto *et al*, 2011). Transient activation of the achaete-scute transcription factor in the ISCs results in the production of EE progenitor cells that can divide further to renew the stem cell and produce pairs of EE cells (Chen *et al*, 2018). The EE population is complex and the different cell subtypes are not fully characterized but two classes (class I and II) of EE cells have been described based

Instituto de Neurociencias, Consejo Superior de Investigaciones Científicas-Universidad Miguel Hernández (CSIC-UMH), Alicante, Spain
*Corresponding author. Tel: +34 965 91 93 90; E-mail: m.dominguez@umh.es
[†]Present address: Institute of Genetics, Heinrich-Heine-University, Düsseldorf, Germany
[‡]Present address: Division of Surgical Research, Department of Surgery, Cooper University Hospital, Camden, NJ, USA
[§]These authors contributed equally to this work
[The copyright line of this article was changed on 30 December 2019 after original online publication.]

on the combination of neuropeptide hormones the EE cell expressed (Beehler-Evans & Micchelli, 2015). Both class I and II of EE cells can be derived from a common stem cell lineage, and the class II cell lineage specification depends on the Notch-Suppressor of Hairless [Su(H)] signalling (Beehler-Evans & Micchelli, 2015). The mechanism that ensures the commitment EBs with activated N and Su(H) signalling towards the EC lineage is not fully understood, and specific tools to label and manipulate the EC-committed EBs have not been characterized thus far.

The homeostatic renewal of the *Drosophila* adult intestine shares many features of more complex animals, and yet, the reduced cell types and the lack of transient amplifying cells allow for a simplified analysis of ISC-production dynamics during homeostasis (Jiang & Edgar, 2012). A typical *Drosophila* ISC divides slowly but continually and produces EBs that can remain incompletely differentiated for long periods in the absence of a local demand for cell renewal (Antonello *et al*, 2015). The existence of such a pool of EBs in homeostatic intestines was first suggested in studies of infection challenge (Buchon *et al*, 2009) but only formally established by multicolour tracing methods (Antonello *et al*, 2015). After infection or genetic induction of EC death (Buchon *et al*, 2009; Jiang *et al*, 2009), the ISC proliferation rate increases to cope with the increased demand for new cells. The mitotic index can increase from 3 to 5 mitoses per midgut to more than 100 mitoses per gut; however, the ISC proliferation rate peaks only 24–48 h *post*challenge (Buchon *et al*, 2009; Jiang *et al*, 2009). During the time interval between challenge and the increase in ISC proliferation, it has been shown that the "pre-existing" EB pool serves as the intestine's first defence (Buchon *et al*, 2009; Antonello *et al*, 2015). A fundamental question is how the stem cell population performs in times of low intestinal demand or how it returns to homeostasis following regeneration of a massive injury since maintaining an "unnecessary" population of immature EBs may increase work load and metabolic demand and thus lead to poorer organ performance or risk of tissue hyperplasia (Zhai *et al*, 2015).

Developing organs often employ a strategy of overproduction followed by culling of the excess cells via programmed cell death (PCD) to ensure correct organ size and shape (Fuchs & Steller, 2011). Although it is counterintuitive that adult stem cells overproduce (i.e. divide superfluously), the importance of apoptosis in maintaining the dynamic numbers and several cell fate specification decisions in the mammalian haematopoietic system has long been defined (reviewed in Oguro & Iwama, 2007), although how haematopoietic stem cells make life and death decisions and the molecular mechanisms involved are incompletely understood. Here, we discovered that ISCs divide in excess of physiological demand and cull excess enteroblast cells via a PCD similar to that which operates during morphogenesis. Execution of cell death involves a conserved axis including Dl-N signalling, the pro-apoptotic transcription factor Klumpfuss/WT and the RUNX homologue Lozenge. This is counteracted by environmental survival signals acting via epidermal growth factor receptor (EGFR) in enteroblast cells, impinging in part on the regulation of the caspase inhibitor Diap1. The gain of genes involved in PCD and the loss of genes involved in survival resulted in a reduction in EB numbers and abrogation of intestinal renewal, whereas blocking caspase genes via a Gal4 line inserted in the *klu* gene, which we show drive expression specifically in the EC-committed enteroblasts, revealed that more than half of the EC-committed progenitor cells produced by the ISCs might be eliminated by PCD in the physiological intestine in conditions of low demand. Furthermore, selective elimination of apoptosis in progenitor cells is sufficient for tumorigenesis to occur. These data provide new insights into the mechanisms of adult tissue homeostasis, opening up new avenues for future investigation of apoptosis and intestinal cancer.

Results

Intestinal stem cells do not adjust their division to slowing intestinal cell replacement

To test whether ISC division adapts to situations of low demand, we developed a "Low" demand protocol to minimize the need for intestinal cell replacement (Fig 1A). The key feature of this protocol is that it minimizes the chances of pathogens accumulating in food, which is the leading cause of EC damage (Apidianakis & Rahme, 2010), by frequently transferring flies to fresh food vials (i.e. 3- to 4-day-old flies were transferred to fresh food vials every 48 h; Fig 1A). To correctly map the fate of progenitor cells, we used the ReDDM ("Repressible Dual Differential Marker": Antonello *et al*, 2015) tracing method, which allows for the unambiguous tracing of stem and progenitor cells and the differentiated progeny. Whereas new ECs are detected as RFP-only cells by the ReDDM-tracing method (Fig 1B), ISCs and/or EBs are detected as double GFP–RFP-labelled cells when using the *esg-Gal4*.

After a temperature shift to inactivate Gal80 (*tub-Gal80^{ts}*), control flies were transferred to fresh vials every week as previously reported (Jiang *et al*, 2009; Antonello *et al*, 2015). As expected from unpredictable fluctuating demands, there was increased renewal of ECs and substantial variation among individual midguts (Fig 1C, empty red bars). This widely used standard culturing condition will be referred to as "Variable" demand. In contrast to these culturing conditions (i.e. new food vial every week) where the intestinal epithelium had renewed completely after 3 weeks (Fig 1C and as previously reported in Antonello *et al*, 2015; Jiang *et al*, 2009), few ECs had renewed at 7, 14 and even 21 days after tracer induction in "Low" demand conditions (*esg^{ReDDM}*-midgut; Fig 1C, solid histogram). Despite the slow epithelial cell turnover in "Low" demand conditions, ISCs continued dividing at a similar rate, producing a similar number of EBs compared to midguts reared in standard culturing conditions (Fig 1C, green histogram). PH3^{+} counts showed that ISCs in "Low" demand maintained a constant proliferation rate (2–5 mitoses/midgut) at days 7, 14 and 21 and compared to the guts of flies in "Variable" demand (Fig 1D). Representative images of guts reared in the standard condition (referred to as "Variable") and a "Low" gut after 2 weeks of tracing are shown in Fig 1E–G. After 3 weeks of tracing, "Low" midguts still had fewer renewed ECs (RFP-only cells) than the "Variable" gut at day 14 (compared Fig 1G and E). No accumulation of EBs was observed in "Low" midguts after 3 weeks of continued ISC division (Fig 1G). This could not be attributed to terminal differentiation because the ReDDM-tracing method detected very few RFP-labelled ECs (Fig 1G and quantification in Fig 1C). This observation prompted us to subsequently investigate whether stem cell production might be regulated by a PCD, in addition to proliferation control.

Blocking apoptosis selectively in ISCs and enteroblasts led to accumulation of undifferentiated progenitor cells and tumour masses

We first drove the expression of the baculovirus caspase inhibitor *p35* in ISCs and EBs of age-synchronized cohorts of adult flies using the esg^{ReDDM} lineage-tracing ReDDM system, and compared with the control, found a significant accumulation of *esg*-positive (*esg*+ve) cells after 7 days ($esg^{ReDDM}>p35$; Fig 1I and H) and the occasional presence of tumour-like masses (Fig 1J). This increase could not be attributed to increased ISC mitosis caused by p35 overexpression (Fig 1K). This revealed that ISCs divide in excess to demand uncovering a hitherto unsuspected role of caspases in the control of stem and/or progenitor cell number. We used the caspase sensor Apoliner, which allows the detection of an even rarer number of apoptotic cells because it marks early steps of apoptosis in which the cell still appears morphologically normal (Bardet *et al*, 2008). To distinguish PCD in progenitor cells from apoptosis-induced aged or damaged ECs and EE cells, we drove *Apoliner* specifically in ISC and EBs using *esg-Gal4*, and in this way, we identified caspase activity to cells with EB morphology (Appendix Fig S1A and B, Antonello *et al*, 2015). This is also consistent with a recent report using an initiator caspase sensor (Baena *et al*, 2018) and unlike earlier caspase-based sensors that detected exclusively activated caspases in enterocytes (Tang *et al*, 2015; Ding *et al*, 2016). These observations hinted at a role for caspases in regulating ISC and/or EB cell

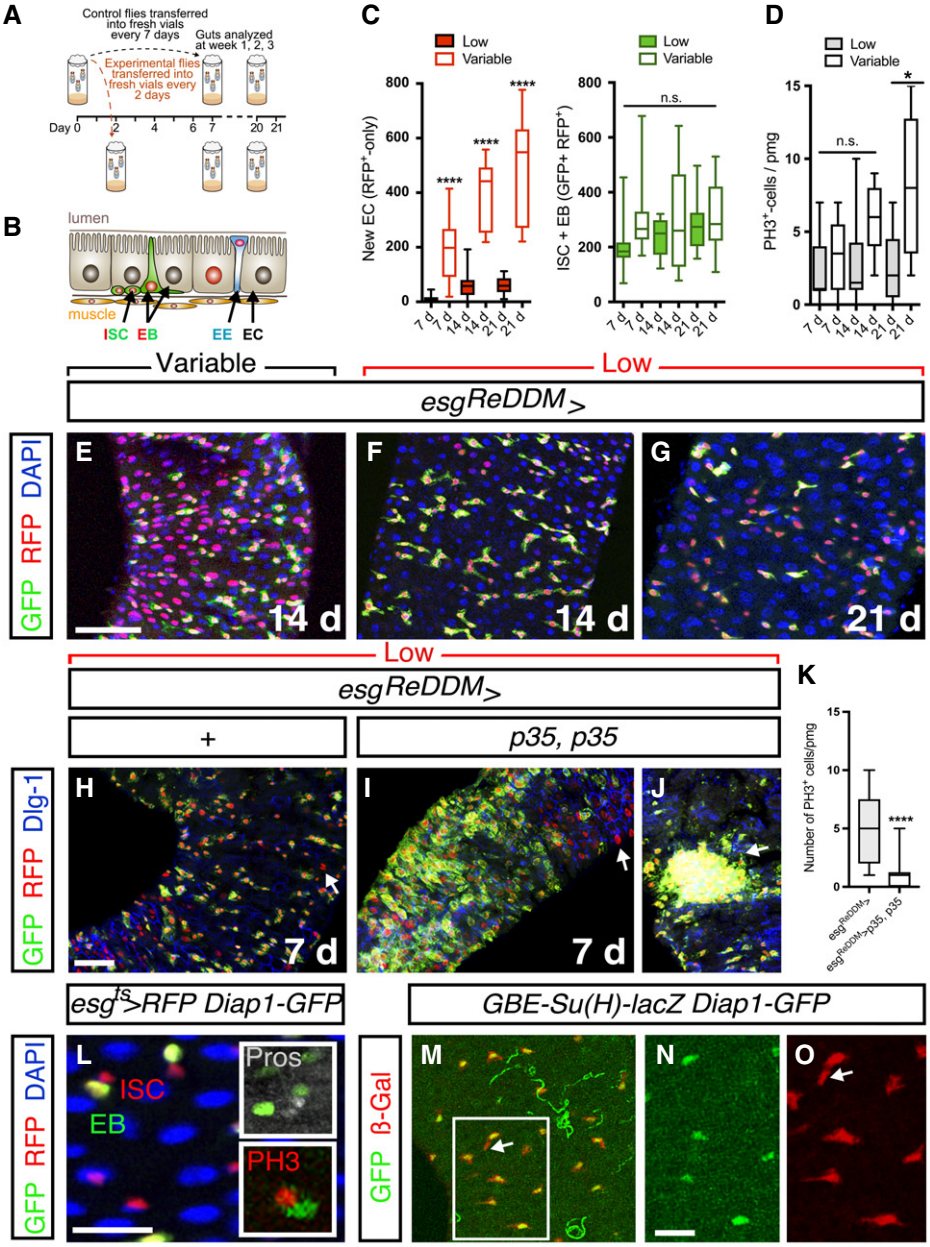

Figure 1.

Figure 1. Inhibition of apoptosis in ISCs and enteroblasts and intestinal expression of Diap1.

A Scheme for tracing intestinal progenitor cell number regulation in midgut with low intestinal renewal ("Low") using the lineage-tracing ReDDM system. The strategy relies on minimizing exposure of flies to contaminated food by transferring flies to fresh food vials every 2 days ("Low") as compared with normal culturing conditions in which flies are typically transferred to fresh food vial every week. This "Low" demand strategy effectively minimized intestinal renewal.

B Scheme of the ReDDM-tracing method (Antonello *et al*, 2015). This system uses two fluorescent transgenes with short-term (membrane CD8::GFP, green) and long-term (nuclear RFP::H2B, red) stability and the Gal80 repressor (*tubα1-Gal80^{ts}*) for temporal control of UAS-driven transgenes. Using *esg-Gal4*, the reporter transgenes are seen in the ISCs and EBs (detected as double-labelled cells). Newly renewed ECs or EEs are traced by the nuclear RFP owing to the protein stability of RFP::H2B.

C Quantification of renewed ECs (RFP-only labelled cells), left graph, and number of ISC and EB cells (double RFP$^+$ GFP$^+$ cells), right graph, in posterior midguts after 7, 14 or 21 days of tracing in normal ("Variable": gut scored n = 9, 8, 4) and low demand ("Low": n = 6, 4, 7) culturing conditions. Asterisks denote significances from one-way ANOVA with Bonferroni's multiple comparison test (**P = 0.0016; ****P < 0.0001).

D Quantification of mitosis (phospho-histone H3 (PH3)$^+$ cells) in low demand midguts at the indicated time points. **P = 0.0015; *n.s.* not significant from one-way ANOVA test.

E Representative adult midgut from control *esg^{ReDDM}* at day 14 after temperature shift in variable demand. ECs renewed are marked positively by persistent RFP labelling (red-only cells).

F, G Few ECs had been renewed in "Low" midguts after 14 (F) and 21 (G) days of tracing.

H–J Age-synchronized posterior midguts of control (*esg^{ReDDM}>*, H) and *p35* overexpression in stem and progenitor cells (*esg^{ReDDM}>p35*, *p35* I and J) at 7 days after temperature shift. Arrows in (H, I) point to newly differentiated ECs. In (J), tumour mass is found in the anterior midgut.

K Quantification of mitosis PH3$^+$ cells in posterior midgut (pmg) (control: gut scored n = 13 and *esg>p35*, *p35*: n = 22]). Student's t-test (****P < 0.0001).

L *Diap1* is monitored by the *GFP.4.3* (green) reporter (Zhang *et al*, 2008; Djiane *et al*, 2013). *Diap1-GFP* is detected in a subset of adult midgut *esg*$^+$ cells that are negative for the mitotic marker PH3 (red, inset) and for EE marker Prospero (Pros, grey in inset). Diap1-GFP is not detected in mature EC (large nuclei cells, DAPI in blue).

M–O Diap1-GFP (green) co-localized almost 100% with the EB marker *GBE-Su(H)-lacZ* (red, M and O). Arrow points to a rare *Diap1-GFP*-negative *GBE-Su(H)-lacZ*-positive cell.

Data information: (E, H, L, N) Scale bars, 50 μm. In the boxplots, the box extends from the 25th to 75th percentiles and whiskers show all points, min to max. The line in the middle of the box is plotted at the median (C, D, K).

numbers. This notion is further reinforced by our functional studies, lineage tracing analysis of a Dronc sensor and analysis of apoptotic progenitor cells using cleaved caspase-3 staining and TUNEL (Terminal Deoxynucleotidyl Transferase (TdT)-mediated dUTP Nick-End Labelling; see Appendix Fig S1C and D and below).

Endogenous Diap1 expression and requirement in enteroblasts

The Diap1 protein (Vasudevan & Don Ryoo, 2015) is crucial for inhibition of caspases (Meier *et al*, 2000). We observed that the *Diap1-GFP4.3* enhancer construct that contains intronic regulatory elements of the *diap1/thread* gene (Zhang *et al*, 2008; Djiane *et al*, 2013) is selectively transcribed in EB cells (Fig 1L–O) as seen by co-staining with the commonly used EB-specific marker *Gbe-Su(H)-lacZ* and ISC markers (Furriols & Bray, 2000; Micchelli & Perrimon, 2006; Zacharioudaki & Bray, 2014). *Diap1-GFP4.3*$^+$ cells were negative for the mitotic marker PH3 and the EE marker Prospero (insets in Fig 1L) and were co-stained with *GBE-Su(H)-lacZ* (Fig 1M; single channel images in Fig 1N and O). We also examined expression of *Diap1* using a *lacZ* enhancer trap in the *Diap1/thread* gene (Ryoo *et al*, 2002) (Appendix Fig S1E–H and J–L). *Diap1-lacZ* signal (Appendix Fig S1E and F) was weakly detected in ISCs, as labelled with anti-Dl (green, Appendix Fig S1G and quantification in M). In contrast, *Diap1-lacZ* signal was strong in EBs as labelled with *NRE-mCherry* (Housden *et al*, 2012) (Appendix Fig S1F and H: quantification in Appendix Fig S1M), indicating that the enhancer elements in the *Diap1-GFP4.3* construct contain *bona fide* regulatory elements for EB expression in the adult intestine. Indeed, Diap1 protein could be detected in the intestine overlapping with the EB marker *NRE-GFP* (Appendix Fig S1I), and *Diap1-GFP* were all co-stained with *Diap1-lacZ* (Appendix Fig S1J and K). *Diap1-lacZ* was also detected at varying levels in some terminally differentiated ECs (Appendix Fig S1K and L) but one cannot rule out that this reflects the perdurance of the stable βgalactosidase protein as seen before with other progenitor-specific *lacZ* reporters (Jiang *et al*, 2009). Thus, *Diap1-GFP* reporter represents a new tool for labelling EBs.

The pro-apoptotic proteins Reaper (Rpr), Head involution defective (Hid) and Grim regulate most apoptotic deaths by counteracting the caspase inhibitor Diap1 (Hirata *et al*, 1995; Meier *et al*, 2000; Holley *et al*, 2002) (scheme, Fig 2A). A Drice-based caspase sensor reporter construct has recently shown that the initiator caspase Dronc is widely activated in the adult intestine (Baena *et al*, 2018). Using the initiator caspase Dronc sensor that is fused to the transcriptional activator QF (act-DBS-S-QF) in combination with *QUAS-Flipase (FLP)* and the *act>FRT-stop>FRT>lacZ* cassette, the cells that activated Dronc and their descendants can be traced over time (Baena *et al*, 2018). Lineage tracing of the intestinal cells that had activated the Dronc are visualized by the presence of βGal labelling (Fig 2B). We found that "Variable" reared guts showed βGal in mature EC cells (large nuclei, DAPI), progenitor cells (small nuclei, Dl-negative cells) and rarely or very low in ISCs (Dl-positive cells; inset in Fig 2B). The lineage tracing activated Dronc cells is consistent with the hypothesis that caspase-mediated apoptosis of EB cells being an integral part of the adult intestinal homeostasis. The fact that many mature EC cells derived from cells that activated Dronc caspase also suggests that EB life/death decisions may depend on the balance between pro- and anti-apoptotic inputs. This is supported by the observations that EB cells also express *Diap1* expression. Thus, we next examined the effect of overexpressing the baculovirus caspase inhibitor *p35* using the commonly used EB-specific driver *GBE-Su(H)-Gal4* (Furriols & Bray, 2000) (Fig 2C), which drive expression in N-specified EB cells. We observed accumulation of clusters of *GBE-Su(H)>GFP*$^+$ cells (Fig 2D), but the phenotype was more variable than that using *esg*-Gal4. Some *GBE-Su(H)>p35, p35* cells show a large size, suggesting also a defect, or a delay, in terminal differentiation (Fig 2D).

Because the *GBE-Su(H)-Gal4* (Furriols & Bray, 2000) also drives expression in class II enteroendocrine progenitors (Beehler-Evans &

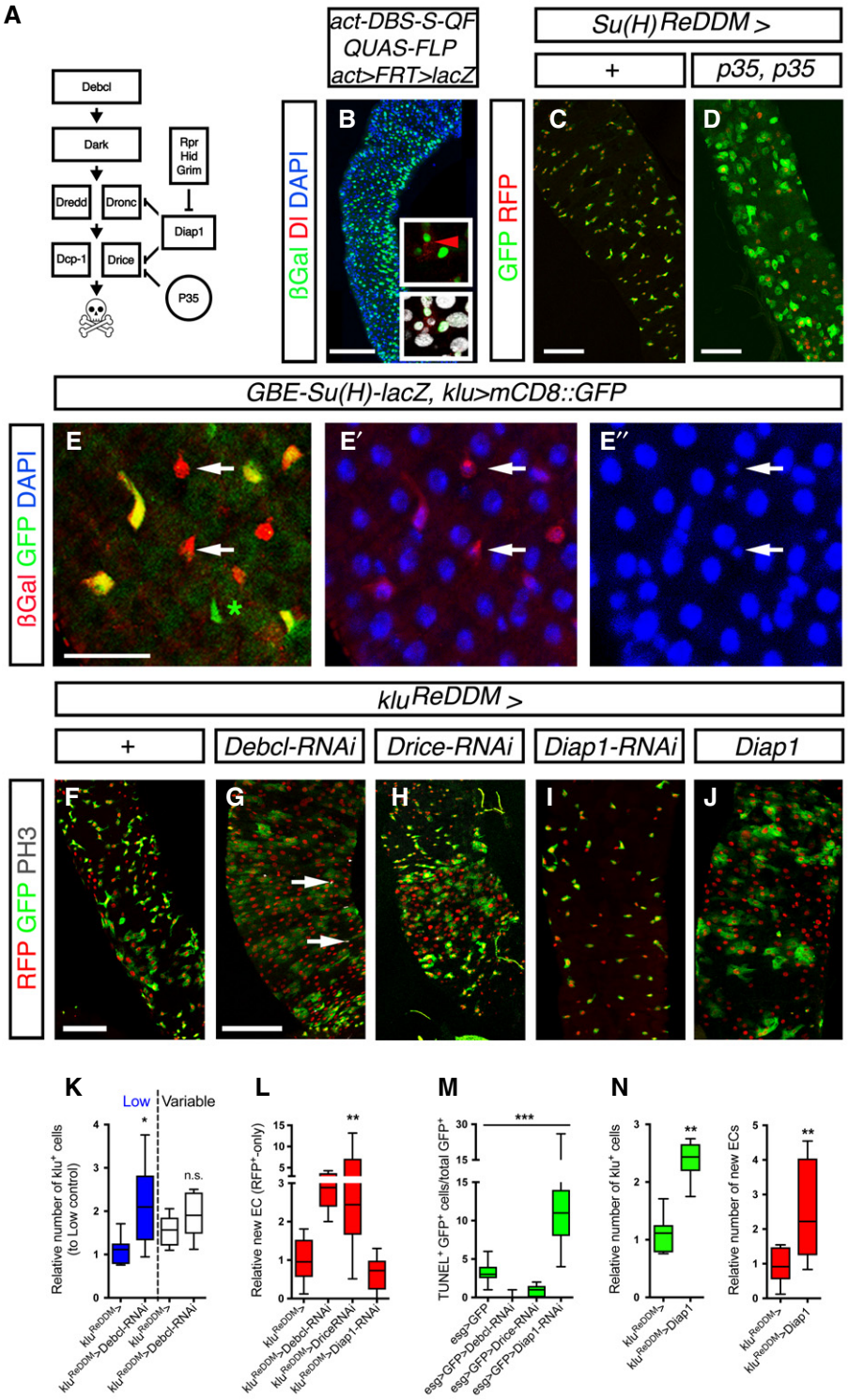

Figure 2.

Micchelli, 2015). *Su(H)*-derived EE progenitor cells can divide and can regenerate the stem cells (Chen *et al*, 2018). Therefore, to understand the homeostatic control of enterocyte (EC)-committed EB cell number by apoptosis, we searched for Gal4 lines that would be specific for those EBs. We found that a Gal4 enhancer trap in the *klu* gene, encoding the *Drosophila* Wilms' Tumour 1 homologue (Klein & Campos-Ortega, 1997), was selectively expressed in this EB population (Fig 2E). This notion is derived from two observations. First, by co-staining midgut carrying *UAS-GFP* and *klu-Gal4* (*klu>GFP*) and the *GBE-Su(H)-lacZ* (Fig 1E) we found that most (81.65% ± 4.66: Mean ± SEM), in $n = 4$ guts) EBs (e.g. cells positive for *GBE-Su(H)* marker) were also positive for *klu>GFP*$^+$.

Figure 2. Physiological caspase-dependent apoptosis of enteroblast cells in the adult midgut.

A Schematic representation of the apoptotic pathway in *Drosophila*.

B Lineage tracing using the initiator caspase sensor *act-DBS-S-QF* (14 days of tracing) combined with *QUAS-FLP* and *act>FRT>lacZ* is visualized by βgalactosidase (βGal, green). ISCs are labelled by anti-Dl (red, insets). Red arrowhead points to the ISC. Gut is counterstained with DAPI (blue) and DAPI (grey, in the inset).

C, D Control *GBE-Su(H)^{ReDDM}>* and (D) *GBE-Su(H)^{ReDDM}>p35, p35* midguts after 7 days of tracing.

E–E″ Adult midgut *klu>mCD8::GFP, GBE-Su(H)-lacZ* stained for β-Gal (red) and GFP (green). DAPI counterstaining in blue (E' and E"). The arrows point to examples of *klu*-negative *Su(H)-lacZ*-positive cells. The green label (asterisk, E) is in the overlying muscle.

F–J Adult midguts of (F) control *klu^{ReDDM}>* (G) *klu^{ReDDM}>Debcl-RNAi*, (H) *klu^{ReDDM}>Drice-RNAi*, (I) *klu^{ReDDM}>Diap1-RNAi*, (J) *klu^{ReDDM}>Diap1* midguts after 7 days of tracing. The arrows point to examples of PH3$^+$ labelled ISCs.

K Quantification of *klu*$^+$ cells in the indicated midguts at day 7 in low demand (Low) or standard (Variable) culturing conditions (n = 7, 5, 9, 7).

L Intestinal cell turnover measured by quantification of the number of newly renewed ECs (RFP-only cells: gut scored n = 9, 13, 9, 13).

M Quantification of apoptotic progenitor cells (*esg*$^+$) measured as GFP$^+$ TUNEL$^+$ cells (n = 9, 9, 9, 9).

N Quantification of *klu*$^+$ cells and renewed ECs in *klu^{ReDDM}>Diap1* posterior midguts (n = 8) relative to "Low" control in (K and L), respectively.

Data information: (K–N) Box and whisker plot showing min to max values and the box is extending from the 25th to 75th percentiles. The line in the middle of the box is plotted at the median. P values (*P < 0.0261; **P < 0.005; ***P < 0.0021) calculated by one-way ANOVA with Bonferroni correction. Scale bars, 100 μm, except in (E), 50 μm.

Around ~15% (14.22% ± 2.504) of *Su(H)*-positive cells were *klu*-negative (Fig 1E′–E″). These EB cells had small nuclei and a round shape, suggesting they represent EE-committed EBs (Beehler-Evans & Micchelli, 2015). Alternatively, these *klu*-negative and *GBE-Su(H)*-positive cells could represent newborn EBs. In such case, the lack of *klu*$^+$ signal could be due to a delay in activation of the binary expression system (*klu-Gal4 UAS-mCD8::GFP*) as compared to the direct expression of *GBE-Su(H)-lacZ* or due to delayed activation of *klu* gene in N-induced EBs. We detected a few instances of *klu*$^+$ (*klu>GFP*$^+$)-positive cells that were negative for *GBE-Su(H)-lacZ* marker (~4.1% ± 2.504), which could be false-negative *lacZ* cells or EB cells that are no longer connected with the ISC and therefore do not maintain *Su(H)* activity. Second, by performing lineage tracing of the *klu-Gal4* (*klu*$^+$) cells using ReDDM system, we found that after two (Appendix Fig S1N) and 3 weeks (Appendix Fig S1O) of the temperature shift 100% of *klu*$^+$-derived cells were of the EC fate and none or very rarely (< 0.2% in 35 midguts) were mature EE cells (summary in Appendix Fig S1P). This indicates that *klu-Gal4* labels EC-committed EBs and that *klu*-negative *Su(H)*-positive EBs are probably EE-committed EBs. This notion has been independently validated by Korzelius *et al* (2019).

We thus used the *klu-Gal4* combined with *ReDDM* system (*klu^{ReDDM}>*, Fig 2F) to assay the effect of endogenous caspase genes in adult midguts by EC-committed EB-selective RNA interference (RNAi)-based silencing of *Debcl* (Death executioner Bcl-2, Fig 2G), *Drice* (Death-related ICE-like caspase, Fig 2H), *Dark* (Death-associated APAF1-related killer, Fig EV1B) and *Dredd* (Death-related ced-3/Nedd2-like caspase, Fig EV1C) in "Low" demand culturing conditions. At day 7, after RNAi transgene induction and tracing, we observed accumulation of EBs and quantification of *Debcl-RNAi* (Fig 2K) revealed a more than twofold increase in *klu*$^+$ cells, which cannot be accounted for by defects in intestinal cell renewal since new ECs (single RFP$^+$ cells) were present in a similar or higher number than in controls (confocal images in midguts in Fig 2F–H and quantification in L).

Silencing of *Diap1* via RNAi (Fig 2I) and its overexpression (Fig 2J) using *klu^{ReDDM}* or the overexpression of its target the caspase *Dronc* (Meier *et al*, 2000) (Fig EV1E and quantification in F) led to the elimination of many *klu*$^+$ cells (Fig 2I) or the accumulation of *klu*$^+$ cells (Fig 2J). Analysis of efficacy of the RNAi transgenes used as measured by qPCR is presented in Fig EV1G.

To further corroborate a role of caspases in regulating EB cell numbers, clonal size of cells mutant for *Drice* was analysed using MARCM method (Fig EV1H). This analysis revealed that *Drice*^{17} mutant clones contained significantly more cells than control WT clones without exhibiting a statistically significant increase in the number of mitosis (Fig EV1H). Together, these data suggest that the homeostatic control of EB cell numbers is regulated by a caspase-dependent process in adult guts. Given the extensive activation of caspase in the adult midgut during normal cell renewal (Fig 2B) and the fact that activated caspases can perform non-apoptotic roles (Baena *et al*, 2018; citations therein), we examined the presence of apoptotic progenitor cells under conditions of RNAi transgene expression using the TUNEL assay, which detects extensive DNA degradation (late stages of apoptosis). Because the TUNEL method led to a strong decay of fluorescent reporters, we could only identify progenitors marked by GFP using *esg-Gal4* combined with GFP antibodies (see Appendix Fig S1C and D) but not using *klu-Gal4* or *Su(H)-Gal4*.

While silencing of the caspases *Debcl* and *Drice* using *esg-Gal4* reduced the number of apoptotic *esg*-positive (*esg*$^+$) cells, silencing *Diap1* or expression of *Dronc* was accompanied by a significant increase in the number of apoptotic *esg*$^+$ cells assayed by the TUNEL method (Fig 2M) and anti-cleaved caspase-3 labelling (Fig EV1F). Conversely, enteroblast-specific overexpression of *Diap1* leads to increased number of progenitor cells (*klu*$^+$ cells) and renewal (Fig 2N). The presence of *esg*$^+$ apoptotic cells along with changes in EB numbers supports the notion that homeostatic ISCs overproduce progenitor cells in relation to demand and that a significant number of those progeny, the EC-committed EBs, are eliminated by apoptosis in low demand situations. We also found that midgut with silenced *Debcl*, but not those with silenced *Drice*, is associated with more mitotic ISCs (Fig EV2A), suggesting that the higher accumulation of *klu*$^+$ cells in *Debcl-RNAi* midguts as compared to *Drice* midguts (Fig 2G and H) may in part be attributed to increased non-autonomous ISC proliferation. This suggests that surviving EB cells may feedback on the mother ISC.

It has been demonstrated that damaging ECs increases ISC proliferation but that this increase does not occur immediately (Buchon *et al*, 2009). Importantly, other authors found that endogenous levels of *diap1* mRNA are increased immediately after damaging ECs and before the number of ISC mitoses is increased (Shaw *et al*, 2010). We hypothesized that when ECs are damaged and thus more

rapidly renewed in the intestine, the occurrence of EB deaths may diminish, given that the risk of EB accumulation is also lower. Such a mechanism allows to quickly dispose of a pool of progenitor cells for a rapid turnover of the damaged EC cells. This hypothesis suggests that PCD in the adult midgut EBs is a dynamic and tuneable process, which is expected to be regulated by mechanisms that also regulate cell differentiation.

Enteroblast life/death decision is governed by opposing Notch and EGFR activity

The PCD is an essential process occurring during development to cull excess or unneeded cells (Baehrecke, 2002; Protzer *et al*, 2008; Mollereau *et al*, 2012). Moreover, overproduction of progenitor cells appears to be a general mechanism to ensure that correct organ size is attained (Mollereau *et al*, 2012). However, PCD is rarely investigated as a mechanism to control the progenitor cell numbers in adult epithelial tissues. Yet, spontaneous apoptosis has long been observed in the murine and human intestine (Potten, 1992) although spontaneous deaths were attributed to faulty or aged ISCs or progenitor cells. More recently, manipulation of the apoptosis genes has been shown to cause an increase in hair follicle stem and/or progenitor cell number in the murine skin (Fuchs *et al*, 2013). Modulation of progenitor cell numbers by PCD has been reported in the adult haematopoietic system (Domen & Weissman, 1999; Oguro & Iwama, 2007). To better understand the process of PCD in the EC-committed EBs, we examined whether caspase-induced cell death in old or damaged EC cells, which makes use of the cell death- and stress-responsive Jun N-terminal Kinase (JNK) cascade and is typically associated with a compensatory proliferation to stimulate cell replacement (Biteau *et al*, 2008; Chen, 2012), is also employed by the PCD we observed in the EBs. We used the *Diap1*-GFP reporter, which serves as a marker of EBs, in tandem with the JNK activity-sensitive reporter TRE-dsRED (Chatterjee & Bohmann, 2012) and did not find any evidence of dsRED$^+$ in EB (Diap1-GFP$^+$) cells (Fig EV2B and C). Indeed, this would be anticipated because JNK-mediated cell death is typically associated with induction of compensatory proliferation to stimulate the renewal of the damaged cells and maintain homeostasis (Raff, 1996). However, the purpose of culling excess but healthy cells is to reduce their number, and at least during development, this type of apoptosis typically occurs without compensatory proliferation.

The regulation of cell numbers by apoptosis often involves the same signalling pathways that regulate proliferation and differentiation in developing organs. As such, the N and EGFR pathways are prime candidates because they often act antagonistically to promote cell life/death decisions during development (Dominguez *et al*, 1998; Protzer *et al*, 2008). Both N (Micchelli & Perrimon, 2006; Ohlstein & Spradling, 2007; Perdigoto *et al*, 2011) and EGFR (Biteau & Jasper, 2011; Jiang *et al*, 2011; Zhai *et al*, 2015) play critical roles in stem cell renewal, EB specification, differentiation and lineage commitment in adult gut homeostasis and regeneration (Biteau & Jasper, 2011; Perdigoto *et al*, 2011; Jiang & Edgar, 2012; Kapuria *et al*, 2012), but their role in EB death/survival has not been explored. We investigated the effect of cell-autonomous manipulations of N and EGFR signalling in EBs using *klu*^{ReDDM} (Fig 3A–E). Changes in EB number were determined by quantifying *klu*$^+$ cells using lineage-tracing ReDDM (Fig 3F), and complemented by assessing cell death within the progenitor cell compartment detected by GFP$^+$ TUNEL$^+$ cells using *esg*^{ReDDM} (Fig 3G). EC renewal (quantified as RFP$^+$-only cells) and non-autonomous effects on stem cells mitosis (PH3$^+$ cells) were also assessed in the *klu*^{ReDDM} guts with altered N and EGFR activity (Fig EV3A and A′).

Both EB-selective overexpression of the dominant negative form of N (Fig 3B) and of a constitutively active allele of EGFR (Fig 3C) led to EB accumulation compared to the control (Fig 3A). Endogenous over-activated N signalling by RNAi silencing of *Hairless* (*H*) (Fig 3D), the main antagonist of N (Bray, 2016), or by expression of a constitutively active N intracellular domain (data not shown) and expression of a dominant negative form of EGFR (Fig 3E), decreased EB number, as assessed by a reduced number of *klu*$^+$ cells (Fig 3F) and increased number of *esg*$^+$ TUNEL$^+$ cells (Fig 3G). Consistently, the loss of EBs caused by gain of N signalling or by *EGFR* inactivation in EBs was rescued by concomitant inhibition of apoptosis via *Debcl-RNAi* expression, also allowing for the new formation of ECs (Fig 3H and I). Previous work has established that activation of EGFR in EBs by EGF-like ligands produced by different intestinal cells in response to damage acts as a paracrine non-autonomous signalling mechanism, stimulating ISC proliferation (Jiang & Edgar, 2009; Biteau & Jasper, 2011; Zhai *et al*, 2015; Chen *et al*, 2016). In agreement with this, we observed that activation of EGFR in EBs using *klu*^{ReDDM} promoted survival and non-autonomously stimulated ISCs division (grey/white label and see extra ISC). ISCs are labelled by Dl marker (inset, Fig 3C)—quantification of mitosis and EC renewal are shown in Fig EV2A. This observation indicated that the massive accumulation of *klu*$^+$ cells in the midguts with constitutive activation of the EGFR pathway in EBs arose by both the suppressed EB death (autonomous effect) and increased ISC divisions (non-autonomous effect). Three ligands, *spitz, keren* and *vein,* have been shown to activate EGFR in the adult intestine (Jiang & Edgar, 2012). Using qPCR, we found that manipulation of N and EGFR activity specifically in EBs led to significant changes in the expression of the three EGF-ligands (Fig EV2D). We also examined endogenous *Diap1* and *klu* expression levels (Fig EV2E) and found that expression of both genes was significantly changed in midguts with EGFR manipulation and, to a lesser extent, in the midguts with loss of Notch signalling driven by *klu-Gal4*, perhaps due to the fact that *klu* gene is a transcriptional target of N signalling. These analyses also revealed an unexpected requirement for EGFR signalling in regulating endogenous *klu* expression (Fig EV2E). Thus, in addition to their documented role in stimulating ISC proliferation and EB differentiation (Jiang & Edgar, 2009; Biteau & Jasper, 2011; Zhai *et al*, 2015), our data illustrate that the activity levels of N and EGFR are also crucial to drive or suppress PCD in EBs. Consistently, we found that gain and loss of N and EGFR were accompanied by increased or reduced apoptotic *esg*$^+$ *GFP*$^+$ as assessed by the TUNEL$^+$ method (Fig 3G), and that these gains and losses are likely attributable to EB life/death decisions (see below).

Dl is the only N ligand acting in adult intestinal homeostasis and regeneration (Ohlstein & Spradling, 2007). ISCs express *Dl*, which in turn suppresses stemness in the neighbouring daughter cell and drives N-mediated progenitor cell commitment towards the EC lineage or class II EE cell lineage. Our data suggest that Dl-mediated activation of N also regulates PCD in EBs. Thus, N and EGFR signalling may counterbalance EB life/death decisions in the adult midgut

along with their crucial role in stem cell self-renewal, proliferation, differentiation and lineage commitment. This model implies that within the same cell, input by N and EGFR may influence alternative cell fates or states, including cell death, maintenance of undifferentiated EB state and terminal differentiation. We hypothesize that EBs not receiving sufficient survival signals (e.g. EGFR^{low}) will be driven to PCD via the pro-apoptotic input by Dl-N signalling, while EBs with low N activation or receiving high anti-apoptotic input (EGFR^{high}) will survive and differentiate or accumulate in the gut in the absence of differentiating input. This view suggests that

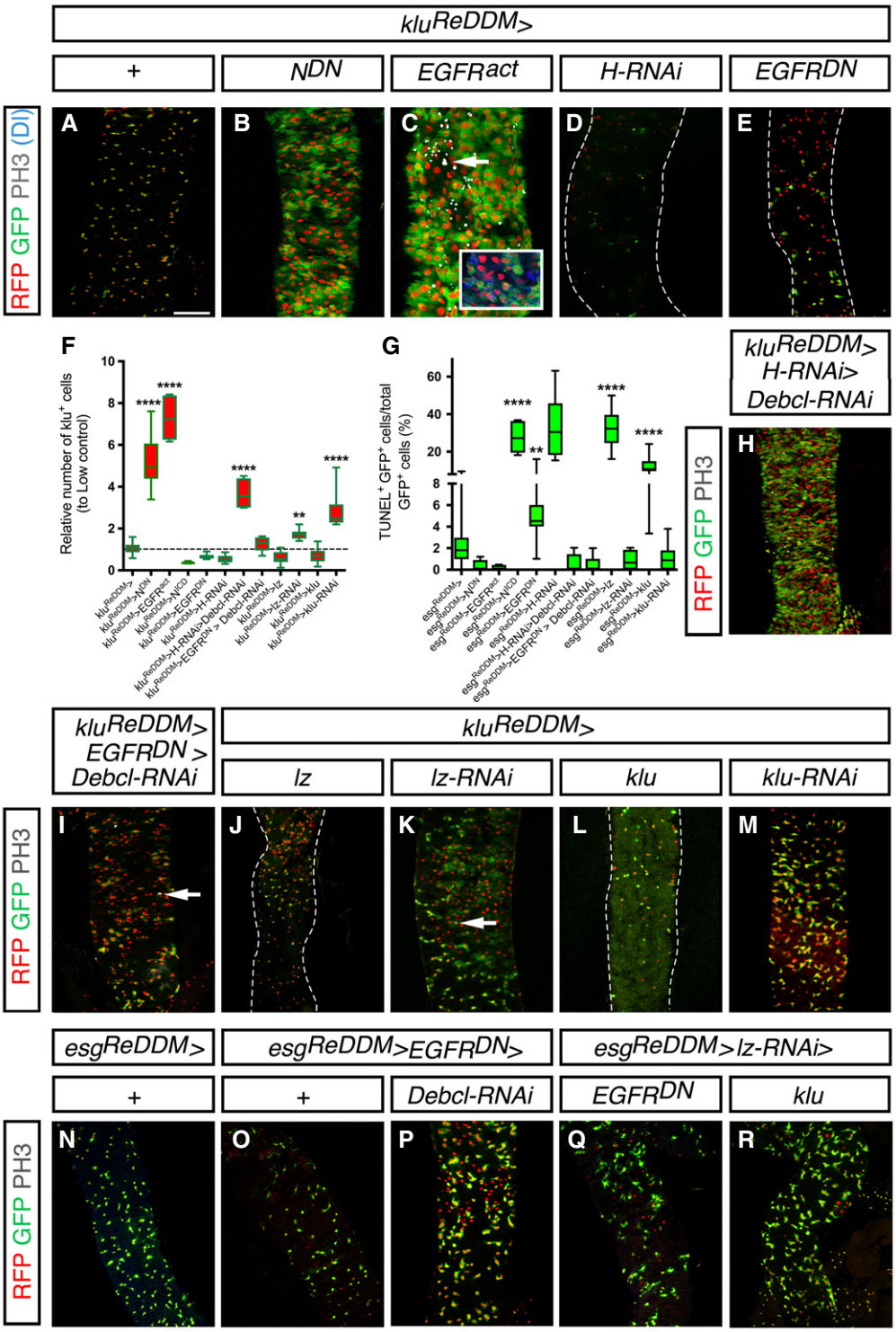

Figure 3.

Figure 3. Enteroblast life and death decision is governed by opposing Notch and EGFR activity.

A–E Confocal images of representative midguts of the indicated genotypes using klu^{ReDDM} for tracing and age- and EB-specific transgene expression at day 7 after temperature shift. ISC mitosis was monitored by using PH3 labelling (white) in all guts. (B–E) Accumulation and loss of klu^{+} cells by loss (B and E) and gain (C and D) of N and EGFR signalling. In (C), the accumulation of EC-committed EBs (klu^{+} cells) in midguts with constitutively activated EGFR ($klu^{ReDDM}> EGFR^{act}$) is accompanied with a non-autonomous increase in ISC mitosis. Inset in (C) shows labelling with Dl (blue), revealing symmetric ISC mitoses as reported previously (Jiang & Edgar, 2009).

F Quantification of the number of klu^{+} (EBs) in the indicated midguts (n = 21, 14, 5, 6, 8, 6, 4, 10, 12, 9, 13, 14).

G Quantification of apoptotic esg^{+} ($TUNEL^{+}$ GFP^{+}) cells in the indicated midguts (n = 28, 4, 7, 7, 16, 8, 8, 7, 10, 7, 20, 24). Quantification of $PH3^{+}$ and EC renewals is in Fig EV2A.

H–M Confocal images of representative midguts of the indicated genotypes as in (A–E). (H and I) Rescue of the loss of EBs induced by gain of Notch (*H-RNAi*) or the loss of EGFR ($EGFR^{DN}$) by expressing *Debcl-RNAi*. (J and K) Impact of gain of expression (J) and loss by RNAi expression (K) of *lz* using klu^{ReDDM} (see Fig EV2A for $PH3^{+}$ quantification). White arrowheads point to examples of mitosis labelled by $PH3^{+}$. (L and M) Impact of gain of expression (L) or loss by RNAi expression (M) of *klu* (M) using klu^{ReDDM}.

N–R Images of representative midguts of esg^{ReDDM} at day 7 after temperature shift of the indicated genotypes. PH3 labelling (white) detected rare mitoses in the mutant genotypes.

Data information: Scale bar, 100 μm for all images. Note that impaired cell renewal reduces the intestinal width. (F, G) $^{**}P < 0.01$; $^{****}P < 0.0001$, one-way ANOVA with Bonferroni correction.

death/life/differentiation may represent a continuum rather than discreet cell fates. This suggests that the individual EB state may change dynamically, while the population of EB remains relatively stable.

The Lozenge and Klumpfuss pro-apoptotic factors regulate the undifferentiated cell culling, cell fate diversification and differentiation rate

Klu/WT is a mediator of PCD during development (Rusconi *et al*, 2004), and we have found that a Gal4 inserted into the *klu* gene is expressed in EC-committed EBs. The RUNX homologue Lozenge (Lz/RUNX) along with Klu/WT1 performs a conserved PCD function (Protzer *et al*, 2008). Therefore, we investigated the role of these two transcriptional regulators in the adult intestine. Using antibodies against the lz/RUNX protein and *lz-Gal4* reporter revealed that the occurrence of lz^{+} cells in a physiological midgut was extremely low (only 1–2 Lz^{+} per posterior midgut; Fig EV2F). Tracing the fate of lz^{+} cells using lz^{ReDDM} showed that they are likely EB "committed" to die as they did not yield differentiated ECs (Fig EV2G). Consistent with this idea, blocking apoptosis via *p35* expression ($lz^{ReDDM}>p35$: Fig EV2H) increased the number of cells derived from lz^{+} progenitors, supporting that *lz* expression may mark EB terminally fated to die. Forcing expression of *lz* in ISCs and EBs using esg^{ReDDM} led to a significant increase in apoptotic esg^{+} cells compared to those obtained by manipulation of N and EGFR ($TUNEL^{+}$ esg^{+}, Fig 3G). Additionally, $esg^{ReDDM}>lz$ midgut also showed precocious terminal differentiation, reflected as small sized ECs (Figs 3J and EV2I). This suggests that Lz/RUNX is downstream of Klu as no enteroendocrine ($Pros^{+}$) cells appear to be traced after *lz* overexpression. When *lz* was depleted via RNAi using klu^{ReDDM} during 7 days, we observed a significant increase in EB number (Fig 3K) and decreased $TUNEL^{+}$ esg^{+} cells (Fig 3G). Quantification of EC turnover showed that EB loss was not due to terminal differentiation (Fig EV2A′) and quantification of $PH3^{+}$ labelling also showed that *lz*-RNAi in EBs in addition to modulate apoptosis it also non-autonomously increases ISC mitosis to a moderate extent (Fig EV2A). This observation is consistent with prior work in the developing fly retina (Behan *et al*, 2002; Siddall *et al*, 2003; Wildonger, 2005), showing that Lz promotes apoptosis through down-regulation of EGFR signalling and thus loss of *lz* leads to increased EGFR activity (see below). Overexpression ($klu^{ReDDM}>klu$; Fig 3L) and depletion of *klu* (and $klu^{ReDDM}>klu\text{-}RNAi$; Fig 3M) also changed EB (klu^{+}) cell numbers, and when expressed by *esg-Gal4,* it also influenced esg^{+} cell death decision as detected by the TUNEL (Fig 3G).

Because mitosis was slightly increased in guts with silenced *lz-RNAi* and *Debcl-RNAi* in EBs, we next attempted to separate the effects of proliferation and that of apoptosis/survival by blocking the feedback loop mediated by EGFR. We thus expressed the $EGFR^{DN}$ transgene using *esg-Gal4* to inhibit EGFR in both stem and EB cells. As previously reported, expression of $EGFR^{DN}$ by *esg-Gal4* led to widespread loss of esg^{+} cells and impaired renewal capacity (e.g. Buchon *et al*, 2009; Jiang & Edgar, 2009) (Fig 3N and O). Strikingly, blocking apoptosis by silencing *Debcl* via RNAi rescued significantly the esg^{+} cell loss and the EC renewal defect caused by $EGFR^{DN}$ (Fig 3P) without rescuing mitosis (quantification in Fig EV2A). Expression of *lz-RNAi* transgene using esg^{ReDDM} partially rescued esg^{+} cell loss by $EGFR^{DN}$ (Fig 3Q), confirming that Lz regulates death/differentiation decisions independent of, or in addition to the cell non-autonomous regulation of ISC proliferation. *Lz*-RNAi expression also suppressed accumulation of EBs triggered by *klu* overexpression (Fig 3R). Conversely, *lz* overexpression (Fig EV2I) could rescue the accumulation of esg^{+} cells caused by $EGFR^{act}$ (Fig EV2J and K). These analyses established that the pro-apoptotic transcriptional regulator Klu acts upstream of Lz, and Lz acts upstream of the caspase inhibitor p35 (Fig EV2H). Collectively, these findings support a N-Klu-Lz and EGFR regulatory network in the regulation of physiological apoptosis during intestinal homeostasis (Fig 4A) in which Lz would be required for the irreversible commitment to death downstream of N-Klu and EGFR, and possibly other factors yet to be defined in the adult *Drosophila* midgut. In EBs with sufficient survival signals, ectopic *lz* expression triggered precocious terminal differentiation. This supports the Lz as a regulator of terminal differentiation.

A role for Klu in sustaining EC fate commitment was also uncovered from *klu-RNAi* experiments using esg^{ReDDM} and klu^{ReDDM} (see Fig EV3). EC fate determination requires the Dl-mediated activation of N signalling in EBs (Perdigoto *et al*, 2011; Kapuria *et al*, 2012). In the absence of N activation, upon stem cell division both daughter cells adopt the ISC fate or terminally differentiate as EE cells, which can be marked by Pros (Jiang & Edgar, 2012). However, in the

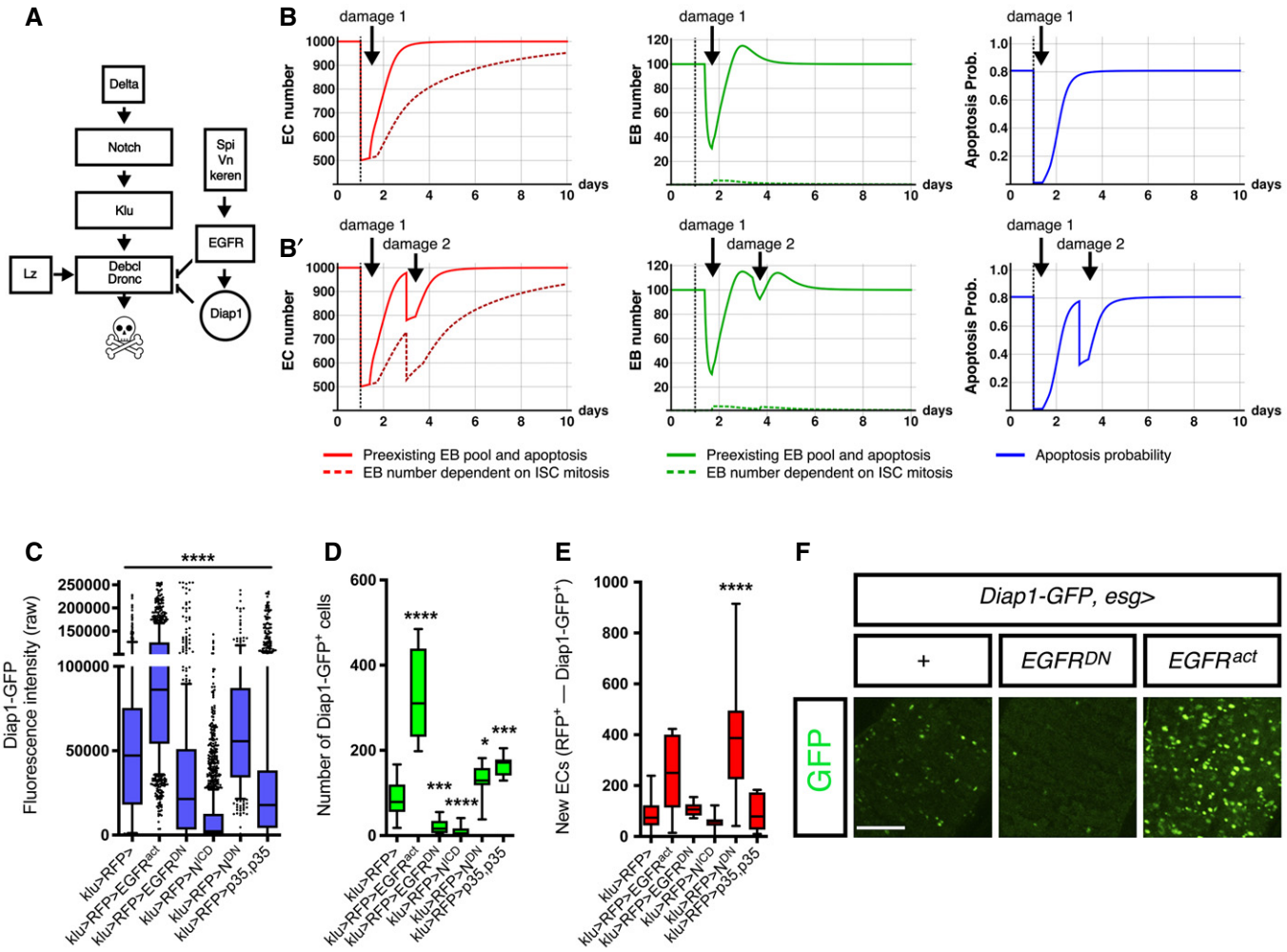

Figure 4. Tuneable apoptosis through tuneable Diap1 signals.

A A model of the regulation of physiological cell death in EC-committed EBs based on our epistatic analysis and previous known gene interactions.

B, B′ Number of ECs over time (left), number of EBs over time (middle) and probabilities of EB loss through apoptosis (right graph). The simulation starts with 1,000 EC cells in all figures (Appendix Supplementary Methods; Appendix Table S1). In (B), a challenge at day 1 imposes a loss of 500 EC cells (black dashed vertical line). In (B′), two successive challenges are imposed: one at day 1, reducing by half the number of ECs (as in B), and a second one at day 3, causing a loss of 200 cells.

C All EBs show Diap1-GFP expression but at varying levels, consistent with EB death fate being tuned by apoptotic input counteracting survival signals.

D Quantification of the number of Diap1-GFP$^+$. Note that in p35-expressing midguts reared in "Low", GFP levels are not increased, consistent with the p35 protein suppressing apoptosis downstream of Diap1.

E Quantification of the number of newly renewed ECs in the indicated genotypes after 7 days. Increase in EB numbers and EC turnover in the EGFR^{act} midgut reflects both suppression of EB deaths and the non-autonomous stimulation of ISC in this background.

F Representative images acquired using the same laser intensity are shown for *Diap1-GFP* in the indicated illustrative examples. Scale bar, 100 μm.

Data information: (C–E) (n = 17, 13, 12, 10, 21, 24). P values were calculated using one-way ANOVA Bonferroni corrected (****P < 0.0001).
Source data are available online for this figure.

presence of high Dl-N signalling, the daughter cell receiving N signalling commits to differentiation towards the EC lineage, which is reflected by the committed progenitor cell increasing its size over time via endoreplication (Perdigoto *et al*, 2011; Lucchetta & Ohlstein, 2012). Dl-N signalling is also required for the specification of a subset of EE cells (Beehler-Evans & Micchelli, 2015). These fate-determination processes are generally depicted as an irreversible commitment. However, we observed that depleting *klu* by RNAi using *klu*^{ReDDM}, which is normal gut will only yield ECs (Fig EV3A and A′), caused in some of the *klu*$^+$ cells a switch of their fate towards the EE lineage (Fig EV3B and C). *klu-RNAi* midguts showed cells with large nuclei (high DNA content shown by DAPI indicate polyploid cells) labelled with Pros (e.g. Fig EV3C), supporting conversion of EC- "committed" EBs towards the EE lineage. Typically, wild-type midguts have a ratio of 10% EEs (Pros$^+$) to 90% ECs (de Navascués *et al*, 2012), and no or rare EE cells were found to be descendants of *klu*$^+$ progenitors (see also lineage tracing in Appendix Fig S1O). However, *klu*-depleted *klu*$^+$ EBs (*klu*^{ReDDM}>*klu-RNAi*, 7 days, Fig EV3D) generated approximately 33% of total EEs instead of 0% (control guts (mean ± SEM) 0.429 ± 0.297 Pros$^+$ RFP$^+$ cells, and *klu*>*klu-RNAi* guts, 98.1 ± 7.21 Pros$^+$ RFP$^+$ cells), indicating a continuous requirement for *Klu* gene expression to

maintain the EC commitment fate. This experiment uncovered an unanticipated plasticity of EBs to adopt an alternative fate. These observations can be interpreted in two alternative models. In one model, Klu^+ activity is required in all EBs for their robust establishment of the EC lineage, as well as the regulation of their number. In the second model, ISCs generate stochastic EC and EE cell fates (~50% EC and ~50% "class II" EE); but N activation could bias the fate towards EC lineage, resulting in more ECs than EE. In such a scenario, Klu^+ would be required to robustly maintain the EC fate in a subset of the EBs, which could account for the observation that EC fate still occurs in $klu^{ReDDM}>klu\text{-}RNAi$ guts. Regardless of the mechanism, these findings are in line with recent studies of mammalian stem cell systems that suggest that progenitor cells are primed, not committed, and cell fate decisions remain tuneable by external inputs (Notta *et al*, 2016).

Comparison of models with a feedback mitosis control and a "tuneable" apoptosis with steady stem cell divisions

Both PCD and stem cell division are energetically costly (Vaux & Korsmeyer, 1999). Thus, to further explore the potential advantages of this apparently costly strategy for adult tissue renewal, we set up a computational model based on these experimental observations to evaluate the performance of a stem cell system in response to injury. We compared a hypothetical system controlling production only by mitosis with a system in which stem cells produce a continuous pool of progenitor cells with further control of their numbers by PCD. The model includes a feedback mechanism by which the steady-state number of EC determines both the rate of ISC division and the probability of EB to undergo either differentiation or apoptosis (Appendix Fig S2). The model predicts a tighter control of the number of ECs under homeostatic conditions and a faster recovery from acute damage (a sudden EC loss for example through injury) (Fig 4B and B′).

A simulated intestinal turnover with single (Fig 4B) and two successive challenges (Fig 4B′) revealed that both models cope with a loss of around 30 ECs per day (Appendix Fig S2), which was the observed average intestinal cell loss in the "Low" demand ReDDM-tracing experiments. However, when we challenged the models with one or two successive acute damages (Fig 4B and B′, respectively), only the model with pre-existing EBs owing to continual ISC divisions predicted a return to homeostasis after 1–2 days after damage consistently with the estimated recovery time determined by previous experimental studies (Amcheslavsky *et al*, 2008; Buchon *et al*, 2009; Jiang & Edgar, 2011).

These simulations hinted at EB death fate in the intestine being a tuneable fate decision presumably by extrinsic cues that also stimulate EB differentiation for cell replacement. Consistent with this idea, we noticed that EBs express a varying level of *Diap1* (assessed by GFP fluorescent intensity, Fig 4C). Importantly, single manipulations of EGFR, N activity or caspase inhibition markedly changed the numbers of $Diap1\text{-}GFP^+$ cells (EBs: Fig 4D; see also quantification of terminal differentiation, new ECs in Fig 4E) along with the *Diap1-GFP* levels as assessed by changes in their fluorescent intensity (Fig 4C) and expression by qPCR (Fig EV2E). The baculovirus *p35* anti-apoptotic factor blocks apoptosis downstream of the *Diap1* transcriptional repression by Rpr/Hid/Grim factors (Hirata *et al*, 1995; Meier *et al*, 2000; Holley *et al*, 2002; Bergmann & Steller, 2009). As anticipated, expression of the *p35* caused accumulation of EBs (Fig 4D) with many of them exhibiting low *Diap1-GFP* levels (Fig 4C). This would suggest that EB cells displaying low *Diap1* levels would normally undergo PCD but escape death by expressing the anti-apoptotic factor *p35*. Importantly, a "tuneable" *Diap1*-GFP is also observed when gene manipulations are done using another promoter, *esg-Gal4* (Fig 4F). Note that EBs with constitutively active EGFR had an excess of EBs but a highly variable Diap1-GFP fluorescence intensity (Fig 4F), suggesting that *Diap1* transcription can be tuned by various signals simultaneously. This is consistent with *Diap1* transcription being directly regulated by several pathways (Zhang *et al*, 2008), most notably the Dl-N pathway itself (Djiane *et al*, 2013) (see also Discussion).

Our observations suggest that adult ISCs overproduce progenitor cells (EBs) probably as a mechanism to respond rapidly to cell damage, and normally compensate this "overproduction" by a culling excess supply via a caspase-dependent death programme that requires N, Klu and Lz upstream of caspases and Diap1, analogous to the PCD that eliminates excess cells during retinal development, e.g. (Baker & Yu, 2001; Bergmann & Steller, 2009). Early findings of spontaneous apoptosis in the human and murine intestinal stem/progenitor cell compartment (Potten, 1992) were attributed to a protection strategy to eliminate damaged or aged stem cells. Our study provides a paradigm for how the apoptotic culling process may operate during cell turnover and how this process is interwoven with proliferation and cell fate determination to ensure that the correct cell types and numbers are produced.

Discussion

We have found that steady-state intestinal stem cell production is not solely controlled by mitosis, but also by a culling process of progenitors. Our observations support a model in which adult ISCs overproduce progenitor cells to ensure rapid intestinal cell renewal in the face of sudden and unpredictable demands, thereby efficiently preserving homeostasis and thus intestinal barrier. Under normal physiological conditions, demand equals supply by ISCs, but in low demand the ISC's production exceeds the tissue demand and EB number is adjusted by a N-Klu-Lz-mediated death via caspase-dependent programme. We have also shown that the elimination of surplus EBs may be also a critical tumour suppressor strategy. Thus, ISC performance both promotes and limits tumorigenesis, and these findings may explain earlier observations of regeneration defects when endogenous inhibitors of apoptosis were impaired (Fuchs *et al*, 2013). Moreover, our epistatic data suggest that Lz acts downstream of Klu and it may mediate cross-talk between N and EGFR to reinforce cell death commitment by dampening EGFR signalling downstream of the receptor (model in Fig 4A) as seen during development (Wildonger, 2005), which may explain how these transcriptional regulators determine robust outcomes of N signalling.

N signalling requires the continuous interaction of the N protein with its membrane-bound ligand Dl in the adjacent stem cells (Ohlstein & Spradling, 2007; Simons & Clevers, 2011; Liang *et al*, 2017). EGFR signalling can be activated in the EB in response to multiple EGF-like signals released by the niche, as well as dying ECs (Liang *et al*, 2017) that also stimulate ISC proliferation, providing

different scenarios for how survival signals may modulate committed progenitor cell numbers. N and EGFR oppositely control life/death decisions in other cellular contexts during development (Baker & Yu, 2001; Gilboa & Lehmann, 2006; Protzer *et al*, 2008). However, in these other developmental contexts apoptosis is highly stereotyped with an invariant outcome and often occurs after cell fate determination. In adult tissues with high and constant demand for cell turnover, the supply of precursor cells needs to be regulated dynamically and adaptively in coordination with cell fate diversification to respond efficiently to changing environmental conditions and with a sudden increase in demand. Indeed, while N and EGFR act oppositely to control the life/death of EBs, they are both positively required for EB terminal differentiation. It is intriguing that Dl-N signalling can directly drive expression of both *rpr* (Krejcí *et al*, 2009) and *Diap1* (Djiane *et al*, 2013). We hypothesize that N activation may "prime" EB to death by activating caspases through induction of pro-apoptotic genes, but simultaneously prevent the execution of the caspase-mediated death programme, which may ultimately depend on the balance of pro-apoptotic and pro-survival or pro-differentiation signals that the EB cells receive. Our data suggest that the balance of pro-apoptotic and pro-survival signals, which may be reflected in the levels of *Diap1* transcription and/or the GFP levels driven by the enhancer elements contained in the *Diap1-GFP4.3*. Caspases appear to be broadly activated in the adult midgut progenitor cells that, depending on level and other input, may perform apoptotic and non-apoptotic roles (Tang *et al*, 2015; Baena *et al*, 2018; and citations therein).

Our data indicate that a "death" signal emanating from the stem cells in direct contact with its committed progeny allows a flexible accommodation of EB number and differentiation to ISC production. We postulate that this "death"/"differentiation" programme may be tuneable by survival/differentiation signals produced by dying cells, from the niche, or other environmental cues, which further attunes EB-number regulation to varying physiological and pathological conditions. In the haematopoietic system, stochastic cell choice provides flexibility for the maintenance of production of all blood cell lineages in the face of substantial demand for one particular lineage (Enver *et al*, 1998). In a speculative manner, we suggest that ISC dividing ahead of demand may similarly generate stochastic cell choice (EC and EE) with a high N-Klu biased fate towards the EC lineage. Derangement of apoptosis-mediated regulation of EB number along with fate conversion may explain the previously observed tumours associated with impaired N signalling (Biteau *et al*, 2011) as supported by our findings (Fig 1J). Similarly, the same mechanism of altered apoptosis within the stem/progenitor cell compartment causes hyperplasia and tumour formation during the murine skin regeneration (Fuchs *et al*, 2013). Our study therefore provides a regulatory logic for the adjustment of progenitor numbers intertwined with both fate diversification and tissue demand.

Materials and Methods

Drosophila stocks and husbandry

The following alleles and fly stocks, as described in Table EV1 and FlyBase (http://flybase.org/), were used:

For ReDDM lineage cell tracing [*UAS-mCD8::GFP, UAS-H2B::RFP, tubα1-Gal80^{ts}*; as described in ref. (Antonello *et al*, 2015)], the following Gal4 drivers were used: *esg-Gal4* (J. Casanova), *klu-Gal4* (T. Klein), *GBE-Su(H)-Gal4* (Zeng *et al*, 2010), *lz-Gal4* (FBtp0099102).

Reporter transgenes: Notch activity-sensitive sensors, *GBE-Su(H)-lacZ* (Furriols & Bray, 2001), the *NRE-EGFP* (FBst0030728) and *NRE-mCherry* [M{NRE-RedRabbit.ins} (FBal0268109) (Housden *et al*, 2012)]; the caspase activity sensor *UAS-Apoliner* (Bardet *et al*, 2008); the initiator caspase Dronc sensor, *act-DBS-S-QF* (gift from Baena *et al*, 2018); the *Diap1-GFP.4.3* (Zhang *et al*, 2008); the *Diap1-lacZ* [*yw; th^{j5C8}/TM3Sb*, *lacZ* enhancer trap in *thread/diap1*; (Ryoo *et al*, 2002)]; the JNK activity sensor, *TRE-DsRed* (Chatterjee & Bohmann, 2012) (FlyBase ID: FBtp0072198, and the Dl-GFP (*Tl{sfGFP}Dl^{GFP}*), a fusion protein generated by CRISPR/Cas9 gene targeting by homologous recombination (Corson *et al*, 2017) (FBal0344893).

Other mutant allele and fly stocks used were as follows: UAS-p35x2 (two insertions, B. Hay), *hsp70-Gal4* (FlyBase ID: FBst0002077), *UAS-Debcl-RNAi* (TRiP.JF02429), *UAS-Dredd-RNAi* (TRiP.HMS00063), *UAS-Drice-RNAi* (TRiP.HMS00398), *UAS-Dark-RNAi* (TRiP.HMS00870), *UAS-Dronc.s* (BDSC:56197, FlyBase ID: FBst0056197), *UAS-Diap1-RNAi* (TRiP.HMS00752), *UAS-klu-RNAi* (TRiP.JF03158), *UAS-N^{DN}* (J. Treisman), *UAS-N^{ICD}* (FlyBase ID: FBal0093233), *UAS-EGFR^{DN}* (FlyBase ID: FBtp0007539), *UAS-EGFR^{act} (EGFR::tor^{act}* (Dominguez *et al*, 1998), *UAS-H-RNAi* (KK104341), *UAS-lz* (FlyBase ID: FBtp0125780), *UAS-N-RNAi* (GD14477), *UAS-lz-RNAi* (TRiP.JF02221), *UAS-klu* (T. Klein), *w^{1118}* (FlyBase ID: FBst0003605). *Actin DBS-S-QF, QUAS-tomato-HA/+*; *QUAS-FLPo* (BL30126)/+; *Actin5C FRT-stop-FRT lacZ-nls/+* (BL6355) (gift from L.A. Baena), *MARCM82* (*hsp70-Flp; tub-Gal4, UAS-mCD8::GFP; FRT{neo FRT}82, tubGal80*) (gift from N. Perrimon).

MARCM clones: The *Drice^{17}* (FBal0219086) clones were induced by combining MARCM (Mosaic Analysis with a repressible Cell Marker system) with *FRT{neo FRT}82B*-containing *Drice^{17}* chromosome (a gift from L.A. Baena). Control (wild type) and *Drice^{17}* clones were induced by a single heat shock of 45 min at 37°C, and adult midguts were analysed at 7 days after clone induction (ACI) and at least 10 clones/midgut were examined in n = 10 adult midguts.

For lineage tracing of the initiator caspase sensor: A Drice-based sensor fused to the transcriptional activator QF (Act-DBS-S-QF) (Baena *et al*, 2018) was combined with the QUAS-FLP transgene and the *flp-out* cassette reporter *Act5c>FRT>stop>FRT>lacZ* (gift from K. Basler). The endogenous activation of the initiator caspase Dronc triggers processing of the Drice-based sensor and ultimately causes the translocation of the transcriptional activator QF to the nucleus. When combined with QUAS-FLP and *act>FRT>stop>FRT>lacZ* construct, lineage tracing of the cells that had activated the Dronc caspase is visualized by the presence of βgalactosidase (βGal) labelling.

Fly crosses were performed at 18°C and reared on standard "Iberian" food. Standard "Iberian" fly food was made by mixing 15 l of water, 0.75 kg of wheat flour, 1 kg of brown sugar, 0.5 kg yeast, 0.17 kg agar, 130 ml of a 5% nipagin solution in ethanol and 130 ml of propionic acid. Upon eclosion, adult female flies of 3–4 days old from control and experimental genotypes were shifted to 29°C in the presence of males and transferred to new food vial every

2 days ("Low" demand condition) or every 7 days ("Variable" demand under standard culturing conditions).

Immunostaining

Adult *Drosophila* midguts were dissected, fixed for 40 min in 4% PFA and stained using the following primary antibodies in PB-T buffer (PBS, 0.1% Triton X-100): rabbit anti-activated caspase3 (1:2,000, Upstate), rabbit anti-PH3 (1:2,000, Upstate), mouse anti-Dlg-1 (1:100, Hybridoma Bank), mouse anti-Pros (1:100, Hybridoma Bank), mouse anti-Dl (1:100, Hybridoma Bank), mouse anti-Lz (1:100, Hybridoma Bank), sheep anti-GFP (1:1,000, Biogenesis), chicken anti-β-Gal (1:1,000, Abcam), anti-Diap1 (1:100, from B. Hay's laboratory) and the according Alexa secondary fluorophore coupled antibodies (1:500, Invitrogen). Nuclei were counterstained with DAPI (Sigma) and mounted in Fluoromount-G (Southern Biotech).

TUNEL assay in stem and progenitor cells

Adult midguts of the indicated genotypes and age were dissected, fixed and immunostained to detect dying GFP-labelled progenitor cells using the *in situ* Cell Death Detection Kit (Roche Applied Science, Grenzach, Germany) according to manufacturer's protocol followed by a DAB reaction (Thermo Fisher, Schwerte, Germany). GFP^+ and $TUNEL^+$ cells were quantified using a Nikon Fluorescence microscope (Eclipse 90i) using brightfield and fluorescence microscopy to count visual fields of 20 × magnification. For NICD midguts, TUNEL was assays 2 days after temperature shift because this manipulation caused rapid cell loss and lethality. Data represent the proportion of $TUNEL^+$ cells relative to total GFP^+ cells. Graphs and all statistical analyses were performed using GraphPad Prism 8, and data were analysed using ANOVA (analysis of variance with Bonferroni correction) statistical test and Student's *t*-tests.

Image acquisition

Confocal images were obtained with a Leica TCS SP5 inverted confocal microscope, using a 1,024 × 1,024 image size. Stacks were typically collected every 1 μm, and the images were reconstructed using max projection. Images were evaluated and scaled using Fiji/ImageJ. In all cases, the images shown in the Figures are representative of the effect of the genetic manipulation.

Quantitative PCR

To assess the efficacy of the RNAi transgenes, mRNA was extracted from wandering third-instar larvae with the corresponding RNAi transgene (*hsp70-Gal4>UAS-RNAi*) or without (control, *hsp70-Gal4>*) after a 1-h heat shock at 37°C to induce transgene expression. To determine mRNA levels, we used superScript First-Strand Synthesis System for RT–PCR (Invitrogen) and SYBR Green PCR Master kit (Applied Biosystems), according to the manufacturer's instructions. The cDNAs were amplified using specific primers designed using the ProbeFinder software by Roche Applied Science, and *RpL32* was used as a house-keeping gene for normalization.

The following primers were used:

Gene	Forward	Reverse
Drice	5′-GTCGGCCCACCCTTAT CTA-3′	5′-TGGACGACCATGACA CACAG-3′
Debcl	5′-ATCATCAACCAGGGGAAATG TCTG-3′	5′-GTTGCGCAAACGCTG TGTC-3′
Diap1	5′-AAATCGTTCATTCTGGTTTT GTTT-3′	5′-GATCTTCCGTCTTATG GACCTATC-3′
H	5′-AACTGTGACCCCAACGT CG-3′	5′-CGAGCTGTTGTCG TCCGAA-3′
lz	5′-TTCACCAGGATCTATTGT GGATGG-3′	5′-ATTGCTCGTGCGCAC CAATTC-3′
keren	5′-CCGCTTTAATCGGCGCTT AC-3′	5′-ATCGGGAAGGTGACA TTCGG-3′
klu	5′-ACCGTCTAAATCAAAGAG TCCCA-3′	5′-TGGCCACAAGATATCC AGCC-3′
N	5′-ACCGTTCGCGGAACTGAT ACC-3′	5′-GCGCAGTAGGTTTTG CCATTG-3′
RpL32	5′-TGTCCTTCCAGCTTCAA GATGACCATC-3′	5′-CTTGGGCTTGCGCCAT TTGTG-3′
spitz	5′-TGCGGTGAAGATAGCC GATC-3′	5′-TTCGCATCGCTGTCCCA TAA-3′
vein	5′-TCCGAGCTAATAGTGCG CTC-3′	5′-TTTATTCTTGGCCCGG CACT-3′

Quantification and statistical analysis, cell counting and fluorescence measurements

For progenitor cell counts, 20× images of ReDDM posterior midguts (pmg, R5) of the different genotypes and conditions were cropped with ImageJ (Fiji 64bit) for processing and quantification with Matlab. A self-written script optimized for the ReDDM method that analyses quality (size, colour) and quantity (count events) in posterior midguts was used to measure the number of progenitor cells (double-positive mCD8::GFP H2B::RFP cells) and DAPI nuclei (Antonello *et al*, 2015).

Measurements of fluorescence intensity of Diap1-lacZ/βGal staining and Diap1-GFP were acquired with a fixed 488 nm laser intensity, and images of midguts were analysed using a Fiji-script for intensity per cell available from the authors. For Diap1-lacZ/βGal quantification in Appendix Fig S1K, intestines were stained with anti-βGal antibody and DAPI. One confocal plane was used to calculate β-Gal fluorescence intensity of nuclear region of interest (ROI) using ImageJ. The ISCs were identified by co-expression of the Dl-GFP enhancer trap (ISCs) and the EBs by the N reporter element NRE-mCherry (NRE-RedRabbit.ins; Housden *et al*, 2012), while enterocytes (ECs) were identified by the exclusive DAPI staining (polyploid, Dl-GFP negative and NRE-mCherry negative). Data were analysed using GraphPad Prism 8. Representative images are shown in all panels. For experiments of the role of apoptosis, at least 20 posterior midguts were scored. For complex experiments analysing many gene conditions, cell counting was usually done in at least four to 10 posterior midguts.

Key resources, antibodies, etc. in Table EV1.

Mathematical model and equations are described in Appendix Supplementary Methods.

Expanded View for this article is available online.

Acknowledgements

We thank T. Klein, P. Adler, K. Dücker, S. Bray, J-P. Vincent, L.A. Baena, H. Herranz, N. Perrimon and B. Hay for reagents; the Bloomington *Drosophila* Stock Center (NIHP400D018537), the Transgenic RNAi Project (TRiP) at Harvard Medical School (NIK/NIGMS R01-GM084947) and the Vienna *Drosophila* Resource Center (VDRC, http://www.vdrc.at) for providing transgenic RNAi fly stocks. We also thank I. Oliveira for technical assistance. T.R. was funded by a postdoctoral Deutsche Forschungsgesellschaft (DFG) fellowship and by a contract by Foundation Botin, and Z.A.A. by a fellowship from MEC-CONSOLIDER. This work in the Dominguez's laboratory was supported by the Spanish Ministry of Economy and Competitiveness and co-financed by FEDER funds (BFU2015-64239-R and "Severo Ochoa" Program for Centers of Excellence in R&C, SEV-2013-0317), the Scientific Foundation of the AECC (Spanish Association Against Cancer) (CICPF16001DOMÍ) and the Valencian Regional Government's Prometeo Programme for research groups of excellence (PROMETEO/2017/146) to M.D.

Author contributions

TR and ZAA performed the majority of experiments and analyses and contributed to the design of the study. EB-I. and LM assisted with the molecular and genetic analysis. SS, MN and LMM developed the computational models. MD provided the general concept, the study design, interpretation, analyses, and supervision, and TR, ZAA and MD wrote the paper.

Conflict of interest

The authors declare that they have no conflict of interest.

References

Amcheslavsky A, Jiang J, Ip YT (2008) Tissue damage-induced intestinal stem cell division in *Drosophila*. *Stem Cell* 4: 49 – 61

Antonello ZA, Reiff T, Ballesta-Illan E, Dominguez M (2015) Robust intestinal homeostasis relies on cellular plasticity in enteroblasts mediated by miR-8-Escargot switch. *EMBO J* 34: 2025 – 2041

Apidianakis Y, Rahme LG (2010) *Drosophila melanogaster* as a model for human intestinal infection and pathology. *Dis Models Mech* 4: 21 – 30

Baehrecke EH (2002) How death shapes life during development. *Nat Rev Mol Cell Biol* 3: 779 – 787

Baena LA, Arthirson L, Bischoff M, Vincent J-P, Alexander C, McGregar R (2018) Novel initiator caspase reporters uncover previously unknown features of caspase-activating cells. *Development* 145: dev170811

Baker NE, Yu SY (2001) The Egf receptor defines domains of cell cycle progression and survival to regulate cell number in the developing *Drosophila* eye. *Cell* 104: 699 – 708

Bardet PL, Kolahgar G, Mynett A, Miguel-Aliaga I, Briscoe J, Meier P, Vincent JP (2008) A fluorescent reporter of caspase activity for live imaging. *Proc Natl Acad Sci USA* 105: 13901 – 13905

Beehler-Evans R, Micchelli CA (2015) Generation of enteroendocrine cell diversity in midgut stem cell lineages. *Development* 142: 654 – 664

Behan KJ, Nichols CD, Cheung TL, Farlow A, Hogan BM, Batterham P, Pollock JA (2002) Yan regulates lozenge during *Drosophila* eye development. *Dev Genes Evol* 212: 267 – 276

Bergmann AA, Steller HH (2009) Apoptosis, stem cells, and tissue regeneration. *Sci Signal* 3: re8

Biteau B, Hochmuth CE, Jasper H (2008) JNK activity in somatic stem cells causes loss of tissue homeostasis in the aging *Drosophila* gut. *Stem Cell* 3: 14 – 14

Biteau B, Jasper H (2011) EGF signaling regulates the proliferation of intestinal stem cells in *Drosophila*. *Development* 138: 1045 – 1055

Biteau B, Hochmuth CE, Jasper H (2011) Maintaining tissue homeostasis: dynamic control of somatic stem cell activity. *Cell Stem Cell* 9: 402 – 411

Bray SJ (2016) Notch signalling in context. *Nature* 17: 722 – 735

Buchon N, Broderick NA, Poidevin M, Pradervand S, Lemaitre B (2009) *Drosophila* intestinal response to bacterial infection: activation of host defense and stem cell proliferation. *Cell Host Microbe* 5: 200 – 211

Chatterjee N, Bohmann D (2012) A versatile ΦC31 based reporter system for measuring AP-1 and Nrf2 signaling in *Drosophila* and in tissue culture. *PLoS ONE* 7: e34063

Chen F (2012) JNK-induced apoptosis, compensatory growth, and cancer stem cells. *Cancer Res* 72: 379 – 386

Chen J, Xu N, Huang H, Cai T, Xi R (2016) A feedback amplification loop between stem cells and their progeny promotes tissue regeneration and tumorigenesis. *Elife* 5: e14330

Chen J, Xu N, Wang C, Huang P, Huang H, Jin Z, Yu Z, Cai T, Jiao R, Xi R (2018) Transient Scute activation via a self-stimulatory loop directs enteroendocrine cell pair specification from self-renewing intestinal stem cells. *Nat Cell Biol* 20: 152 – 161

Corson F, Couturier L, Rouault H, Mazouni K, Schweisguth F (2017) Self-organized Notch dynamics generate stereotyped sensory organ patterns in *Drosophila*. *Science* 356: eaai7407

Ding AX, Sun G, Argaw YG, Wong JO, Easwaran S, Montell DJ (2016) CasExpress reveals widespread and diverse patterns of cell survival of caspase-3 activation during development *in vivo*. *Elife* 5: e10936

Djiane A, Krejčí A, Bernard F, Fexova S, Millen K, Bray SJ (2013) Dissecting the mechanisms of Notch induced hyperplasia. *EMBO J* 32: 60 – 71

Domen JJ, Weissman ILI (1999) Self-renewal, differentiation or death: regulation and manipulation of hematopoietic stem cell fate. *Mol Med Today* 5: 201 – 208

Dominguez M, Wasserman JD, Freeman M (1998) Multiple functions of the EGF receptor in *Drosophila* eye development. *Curr Biol* 8: 1039 – 1048

Enver TT, Heyworth CMC, Dexter TMT (1998) Do stem cells play dice? *Blood* 92: 348 – 352

Fuchs Y, Steller H (2011) Programmed cell death in animal development and disease. *Cell* 147: 742 – 758

Fuchs Y, Brown S, Gorenc T, Rodriguez J, Fuchs E, Steller H (2013) Sept4/ARTS regulates stem cell apoptosis and skin regeneration. *Science* 341: 286 – 289

Furriols M, Bray S (2000) Dissecting the mechanisms of suppressor of hairless function. *Dev Biol* 227: 520 – 532

Furriols M, Bray S (2001) A model Notch response element detects Suppressor of Hairless-dependent molecular switch. *Curr Biol* 11: 60 – 64

Gilboa L, Lehmann R (2006) Soma-germline interactions coordinate homeostasis and growth in the *Drosophila* gonad. *Nature* 443: 97 – 100

Hirata J, Nakagoshi H, Nabeshima Y, Matsuzaki F (1995) Asymmetric segregation of the homeodomain protein Prospero during *Drosophila* development. *Nature* 377: 627 – 630

Holley CL, Olson MR, Colón-Ramos DA, Kornbluth S (2002) Reaper eliminates IAP proteins through stimulated IAP degradation and generalized translational inhibition. *Nat Cell Biol* 4: 439 – 444

Housden BE, Millen K, Bray SJ (2012) Drosophila reporter vectors compatible with ΦC31 integrase transgenesis techniques and their use to generate new notch reporter fly lines. *G3* 2: 79 – 82

Jiang H, Edgar BA (2009) EGFR signaling regulates the proliferation of *Drosophila* adult midgut progenitors. *Development* 136: 483 – 493

Jiang H, Patel PH, Kohlmaier A, Grenley MO, McEwen DG, Edgar BA (2009) Cytokine/Jak/Stat signaling mediates regeneration and homeostasis in the *Drosophila* midgut. *Cell* 137: 1343 – 1355

Jiang H, Edgar BA (2011) Intestinal stem cells in the adult *Drosophila* midgut. *Exp Cell Res* 317: 2780 – 2788

Jiang H, Grenley MO, Bravo MJ, Blumhagen RZ, Edgar BA (2011) EGFR/Ras/MAPK signaling mediates adult midgut epithelial homeostasis and regeneration in *Drosophila*. *Stem Cell* 8: 84 – 95

Jiang H, Edgar BA (2012) Intestinal stem cell function in *Drosophila* and mice. *Curr Opin Genet Dev* 22: 354 – 360

Kapuria SS, Karpac JJ, Biteau BB, Hwangbo DD, Jasper HH (2012) Notch-mediated suppression of TSC2 expression regulates cell differentiation in the *Drosophila* intestinal stem cell lineage. *PLoS Genet* 8: e1003045

Klein TT, Campos-Ortega JAJ (1997) klumpfuss, a *Drosophila* gene encoding a member of the EGR family of transcription factors, is involved in bristle and leg development. *Development* 124: 3123 – 3134

Korzelius J, Ronnen-Oron T, Baldauf M, Meier E, Sousa-Victor P, Jasper H (2019) The WT1-like transcription factor Klumpfuss maintains lineage commitment in the intestine. *Nat Commun* 10: 4123

Krejcí A, Bernard F, Housden BE, Collins S, Bray SJ (2009) Direct response to Notch activation: signaling crostalk and incoherent logic. *Sci Signal* 2: ra1

Liang J, Balachandra S, Ngo S, O'Brien LE (2017) Feedback regulation of steady-state epithelial turnover and organ size. *Nature* 548: 588 – 591

Lucchetta EM, Ohlstein B (2012) The *Drosophila* midgut: a model for stem cell driven tissue regeneration. *Wiley Interdiscip Rev Dev Biol* 1: 781 – 788

Meier P, Silke J, Leevers SJ, Evan GI (2000) The *Drosophila* caspase DRONC is regulated by DIAP1. *EMBO J* 19: 598 – 611

Micchelli CA, Perrimon N (2006) Evidence that stem cells reside in the adult *Drosophila* midgut epithelium. *Nature* 439: 475 – 479

Mollereau B, Perez-Garijo A, Bergmann A, Miura M, Gerlitz O, Ryoo HD, Steller H, Morata G (2012) Compensatory proliferation and apoptosis-induced proliferation: a need for clarification. *Cell Death Differ* 20: 181 – 181

de Navascués J, Perdigoto CN, Bian Y, Schneider MH, Bardin AJ, Martinez Arias A, Simons BD (2012) *Drosophila* midgut homeostasis involves neutral competition between symmetrically dividing intestinal stem cells. *EMBO J* 31: 2473 – 2485

Notta F, Zandi S, Takayama N, Dobson S, Gan OI, Wilson G, Kaufmann KB, McLeod J, Laurenti E, Dunant CF *et al* (2016) Distinct routes of lineage development reshape the human blood hierarchy across ontogeny. *Science* 351: aab2116

O'Brien LE, Soliman SS, Li X, Bilder D (2011) Altered modes of stem cell division drive adaptive intestinal growth. *Cell* 147: 603 – 614

Oguro H, Iwama A (2007) Life and death in haematopoietic stem cells. *Curr Opin Immunol* 19: 503 – 509

Ohlstein B, Spradling A (2006) The adult *Drosophila* posterior midgut is maintained by pluripotent stem cells. *Nature* 439: 470 – 474

Ohlstein B, Spradling A (2007) Multipotent *Drosophila* intestinal stem cells specify daughter cell fates by differential notch signaling. *Science* 315: 988 – 992

Parasram K, Bernardon N, Hammoud M, Chang H, He L, Perrimon N, Karpowicz P (2018) Intestinal stem cells exhibit conditional circadian clock function. *Stem Cell Rep* 13: 1287 – 1301

Perdigoto CN, Schweisguth F, Bardin AJ (2011) Distinct levels of Notch activity for commitment and terminal differentiation of stem cells in the adult fly intestine. *Development* 138: 4585 – 4595

Potten CS (1992) The significance of spontaneous and induced apoptosis in the gastrointestinal tract of mice. *Cancer Metast Rev* 11: 179 – 195

Protzer CE, Wech I, Nagel AC (2008) Hairless induces cell death by downregulation of EGFR signalling activity. *J Cell Sci* 121: 3167 – 3176

Raff MC (1996) Size control: the regulation of cell numbers in animal development. *Cell* 86: 173 – 175

Rusconi JC, Fink JL, Cagan R (2004) klumpfuss regulates cell death in the *Drosophila* retina. *Mech Dev* 121: 537 – 546

Ryoo HD, Bergmann A, Gonen H, Ciechanover A, Steller H (2002) Regulation of *Drosophila* IAP1 degradation and apoptosis by reaper and ubcD1. *Nat Cell Biol* 4: 32 – 438

Sallé J, Gervais L, Boumard B, Stefanutti M, Siudeja K, Bardin AJ (2017) Intrinsic regulation of enteroendocrine fate by Numb. *EMBO J* 36: 1928 – 1945

Shaw RL, Kohlmaier A, Polesello C, Veelken C, Edgar BA, Tapon N (2010) The Hippo pathway regulates intestinal stem cell proliferation during *Drosophila* adult midgut regeneration. *Development* 137: 4147 – 4158

Siddall NAN, Behan KJK, Crew JRJ, Cheung TLT, Fair JAJ, Batterham PP, Pollock JAJ (2003) Mutations in lozenge and D-Pax2 invoke ectopic patterned cell death in the developing *Drosophila* eye using distinct mechanisms. *Dev Genes Evol* 213: 107 – 119

Simons BD, Clevers H (2011) Stem cell self-renewal in intestinal crypt. *Exp Cell Res* 317: 2719 – 2724

Tang HL, Tang HM, Fung MC, Hardwick JM (2015) *In vivo* CaspaseTracker biosensor system for detecting anastasis and non-apoptotic caspase activity. *Sci Rep* 5: 9015

Vasudevan D, Don Ryoo H (2015) Regulation of cell death by IAPs and their antagonists. *Curr Top Dev Biol* 114: 185 – 208

Vaux DL, Korsmeyer SJ (1999) Cell death in development. *Cell* 96: 245 – 254

Wildonger J (2005) Lozenge directly activates argos and klumpfuss to regulate programmed cell death. *Genes Dev* 19: 1034 – 1039

Zacharioudaki E, Bray SJ (2014) Tools and methods for studying Notch signaling in *Drosophila melanogaster*. *Methods* 68: 173 – 182

Zeng X, Chauhan C, Hou SX (2010) Characterization of midgut stem cell- and enteroblast-specific Gal4 lines in *Drosophila*. *Genesis* 48: 607 – 611

Zhai Z, Kondo S, Ha N, Boquete J-P, Brunner M, Ueda R, Lemaitre B (2015) Accumulation of differentiating intestinal stem cell progenies drives tumorigenesis. *Nat Comms* 6: 10219

Zhang L, Ren F, Zhang Q, Chen Y, Wang B, Jiang J (2008) The TEAD/TEF family of transcription factor scalloped mediates hippo signaling in organ size control. *Dev Cell* 14: 377 – 387